

EXPERIMENTAL STUDY ON ELECTROHYDRODYNAMIC HEAT TRANSFER ENHANCEMENT OF SEMICIRCULAR RIBS INTO CHANNEL

by

Amin ALAMI nia^{a*}, Tohid KHEIRI^a and Moharram JAFARI^b

^aDepartment of Mechanical Engineering, Azarbaijan Shahid Madani University, Tabriz, Iran

^bDepartment of Mechanical Engineering, The University of Tabriz, Tabriz, Iran

Original scientific paper

<https://doi.org/10.2298/TSCI161024201A>

In this study, the heat transfer enhancement on semicircular ribs established on the floor of rectangular duct is investigated. These ribs were used as heat sources and cooling of them has been achieved with electrohydrodynamic (EHD) active method by experimental procedure. The flow was 3-D, steady, viscous and incompressible with regimes of both laminar and turbulent ($500 \leq Re_{D_h} \leq 4500$). The hydrodynamics and heat transfer behavior of the air-flow was studied by EHD active method with application of corona wind. The aim of this work is application of EHD active method for convective heat transfer enhancement. In this method, two arrangements of wire electrodes have been achieved. The results show that in same Reynolds numbers and voltages of wire electrodes, the heat transfer enhancement was increase in Arrangement 1 than Arrangement 2.

Key words: convection, enhancement, ribs, electrohydrodynamic, corona wind

Introduction

Cooling of hot electronic board surfaces and other local heat sources with air-flow is an essential part of the boards and heating systems. The main cooling systems for these equipments are flowing of air over them through channels, thus reducing heat generation through forced convection. Active methods are well known for their ability to work with external sources of energy. The active method with application of corona wind is well known owing to its ability to work with any external sources of energy. Corona is a visible luminous emission caused by the creation of photon and occurs in the vicinity of sharp edges where the intensity of the electric field is high. An important aspect of corona discharge is the generation of corona wind, which is a gas-flow induced by corona discharge. This phenomenon is caused by the ionization of gas molecules and formation of electrons that accelerate in strong electric fields and collide with neutral molecules, resulting in more ionization. Because the ions are heavier than electrons, they accelerate and drag the neighboring gas molecules. This action generates a secondary flow, known as corona wind. The present work examines active methods of the cooling system. The active cooling system is a new cooling method, which has been developed in our lab with construction of apparatus.

The present work examines an active EHD method with application of positive corona wind for the cooling of heat generating semi circular ribs placed at the base of channel.

Alamgholilou and Esmaeilzadeh [1], investigated experimental study on the heat transfer enhancement of rectangular ribs with constant heat flux located in the floor of a rect-

* Corresponding author, e-mail: amin.alam@azaruniv.ac.ir

angular channel. In this study, the behavior of air-flow was studied by passive, active and compound methods. The comparison of the results for various boundary conditions of problem was fairly agreement. Alamgholilou and Esmailzadeh [2] and Esmailzadeh and Alamgholilou [3], investigated numerical study on the heat transfer enhancement of rectangular ribs with constant heat flux located in the floor of a 3-D duct flow has been achieved. In this study, the effects of the arranged holes between the rectangular ribs in channels have been reported.

Alami nia and Campo [4, 5], investigated 3-D and 2-D experimental study on the heat transfer enhancement of semi circular ribs with constant heat flux located in the floor of a rectangular channel has been achieved. In this study, the behavior of air-flow was studied by active EHD method. The results show that in same Reynolds numbers and voltages of wires, the heat transfer enhancement was increased in best arrangement than other arrangements. Density of electric charge around of wire electrodes in best arrangement is higher than other arrangements.

Sultan [6] indicated an enhancement in heat transfer by inducing distributions in vortices due to existence of holes behind the ribs with passive method of heat transfer enhancement in channel. But in analysis of fluid motion in wake region he considered the effect of density variation and buoyancy forces. According to the negligible Richardson number of flow, buoyancy forces contribute minor role in this phenomenon. In addition in definition of critical Reynolds a specified characteristic length was established which is not appropriate with geometry and physical model of this case. Applying repeated ribs and their distances from each other in channel or in external flow on plain surfaces can influence patterns of flow field.

Fujishima *et al.* [7] provided analyzed the flow interaction between the primary flow and the secondary flow in the wire-duct electrostatic precipitator. They extended to incorporate the alternately oriented point corona on the wire-plate type electrodes.

Ohadi *et al.* [8] used the wire-plate electrodes for forced convection enhancement in pipe flow. They showed that the two-wire electrode design provided a modest higher enhancement compared to the single wire electrode design. With two electrodes, they showed that for Reynolds numbers up to 10000, it is possible to use this technique for enhancement.

Kasayapanand and Kiatsiririot [9, 10] investigated the heat transfer enhancement with the EHD technique in laminar forced convection inside a wavy channel with different wire electrode arrangements. The electric field is generated by the wire electrodes charged with DC high voltage. The mathematical modeling includes the interactions among the electric, flow and temperature fields. The numerical simulation was firstly applied to the rectangular flat channel and later to wavy channel.

Kasayapanand *et al.* [11] investigated the effect of the electrode arrangements in a tube bank with regards to the characteristic of EHD heat transfer enhancement for low Reynolds numbers. The numerical modeling of the laminar forced convection includes the interactions among the electric field, the flow field, and the temperature field. From the numerical results, they showed that the heat transfer was enhanced by the EHD at a low Reynolds number and the short distance between the wire electrodes and the tube surface.

Shooshtari *et al.* [12] investigated the EHD enhancement of heat transfer in air laminar channel flow. They showed that the heat transfer was enhanced by the EHD at a low Reynolds numbers.

Tada *et al.* [13] investigated the heat transfer enhancement in a convective field by applying ionic wind. They showed that the heat transfer was enhanced by the effects of ionic wind with application of EHD.

Often times in thermal systems, invigorating the heat transfer rate cause deterioration in the momentum transfer. This phenomenon is called dissimilarity. At first by placing semi cir-

cular ribs in the floor channel, local pressure and momentum both drop. Therefore, for a specified inlet velocity situation, more pumping power is needed. On the other hand, due to the local effects such as disturbance and the extending of contact surface, the heat transfer increases. So it is necessary to articulate a convenient similarity between these two opposing phenomena. By using a suitable active method, secondary flow of corona wind creates in space between semi circular ribs and causes disturbances. In the present work, to avoid immoderate changes in the physical properties of fluid, the temperature differences between the fluid and semi circular ribs are constrained by applying a convenient heat flux on the semi circular ribs.

Experimental investigation

In order to generate data of the air-flow patterns around the semi circular ribs, a special apparatus was necessary. In designing the test section, the following conditions were taken into consideration:

A fully developed air-flow should be supplied before the flow enters into the test section. With regards to the dimensions of the channel, the depth to height ratio is high. Because the depth effects have been ignored the channel is 2-D. The apparatus is designed to flow with low and large values of Reynolds numbers under laminar and turbulent ($500 \leq Re_{Dh} \leq 4500$) regimes. The flow is incompressible with very small mach numbers, $M \ll 0.3$. Thus any interaction effects of high voltage electric fields on the measurement of temperature are due to the eliminating side effects of applied high voltage. Therefore, for increase on accuracy of thermocouples, a strength dielectric barrier discharge was used.

Figure 1 shows the schematic and the layout of the main experimental apparatus. By considering the aforementioned conditions for the main experimental section, a special experimental apparatus was designed for the investigation of heat transfer enhancements involving semi circular ribs to fluid. For this purpose, a broad rectangular channel was used. To measure the volume rate of air-flow, the orifice meter was used. The ratio in diameter (orifice to pipe) was adjusted to be $\beta = d/D = 0.25$. A special centrifugal fan was used to produce the air-flow. To eliminate disturbances, the test section was located on the suction side of the fan. Figure 2 shows the photograph of the main experimental apparatus.

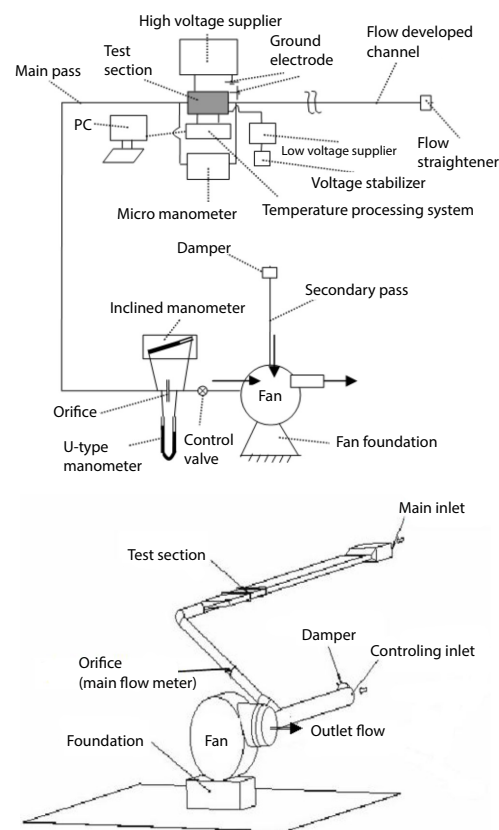


Figure 1. The schematic and the layout of main apparatus

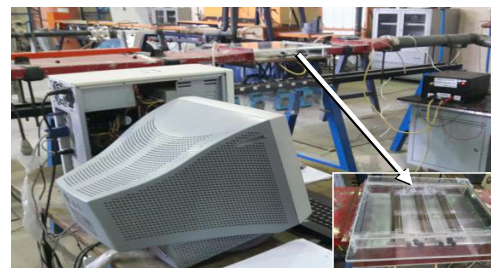


Figure 2. Photograph of the main set-up

The test section was designed to be a channel with 40 cm length, $H = 4$ cm height, and $W = 30$ cm width as shown in fig. 3. Before entering the test section flows from a rectangular channel with 2 m length, the fluid proceeds with a rectangular flow-straightened screen with unit dimension of 8-20 mm. The velocity domain in the test section was $0.11 \leq u \leq 1$ m/s. The hydraulic diameter of the main channel (especially the test section) was 7.06 cm.

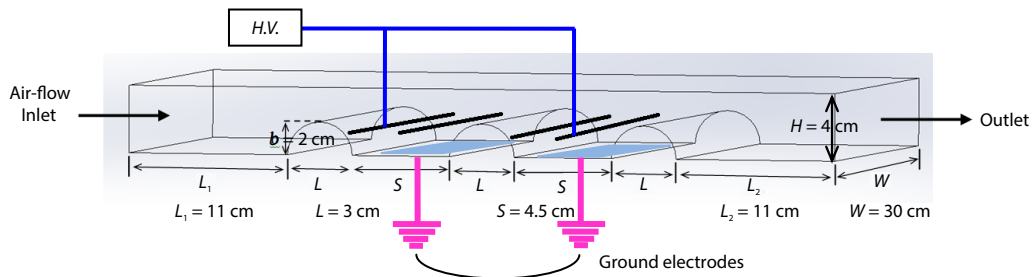


Figure 3. Schematic and geometry of the test section

The fan was adjusted to operate with constant rotation. The flow rate was measured by the orifice meter under the France standard NF X 10-102 [14]. The pressure measurements should be determined with high accuracy in the two sides of the orifice. In the current study, a U-type manometer with Kerosene ($SG = 0.865$) was used (SG is specific gravity). In the test section, the ribs were electrically heated with constant heat flux. To isolate the part attached to the floor of the channel, a fire proof fiber was used. The fire proof fiber is an adequate insulator of heat and electricity. The semi circular ribs were produced using silicon iron foil. Three semi circular ribs were attached on the floor of the channel. The series were connected as resistance to provide a constant heat flux of $q_w'' = 4500$ W/m² by means of a differential voltage transformer. The semi circular ribs had in width, 30 cm in length and 3 cm in axial spacing between them. The 22 thermocouples were used for measuring the temperature of the bottom channel wall and the ribbons surface in central direction of flow. The type of thermocouples is T-type with Cu-Constantan. The geometric layout of thermocouples in the test section is shown in fig. 4, where x denotes the stream wise direction from the position of the first thermocouple in the test section. The x location of the thermocouples is determined in the best location for measuring the temperature. The position of thermocouples (x location of thermocouples) is increased on surfaces of the ribs. This position starts from the first semi circular rib to thermocouple Number 22. The thermocouple Number 1 is used for measuring the ambient air temperature.

For temperature processing, the ADAM digital system was used. This system contains four boards for temperature measurement and a transformation board. Each measuring board receives the information of thermocouples and then transfers them to the PC for processing.

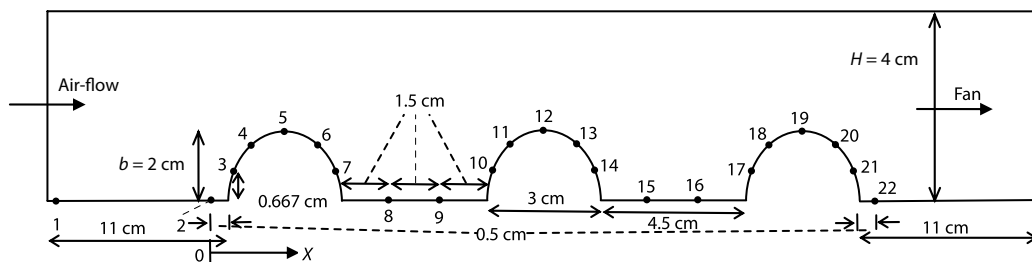


Figure 4. The thermocouples arrangement

High voltage is applied using a high voltage supplier for the EHD wire-plate active method. Various arrangements of wire and plates were made as ground electrodes were designed between the spacing of the semi circular ribs. The high voltage supplier generated voltages up to 40 kV between the wire and ground electrodes. The corona phenomenon was generated between electrodes with very weak current intensity. The micro-ammeter is used for current intensity measurements with a domain of 0-500 μA and accuracy of 10 μA . In all experimental tests, the polarity of wire electrodes is positive. The diameter of wire electrodes is 0.6 mm. The wire and ground electrodes are made from Cu and Al, respectively. The primary objective of the present work is the comparison of plain Case 1 with EHD active heat transfer enhancement method. The geometry of the two cases is shown in figs. 5(a) and 5(b).

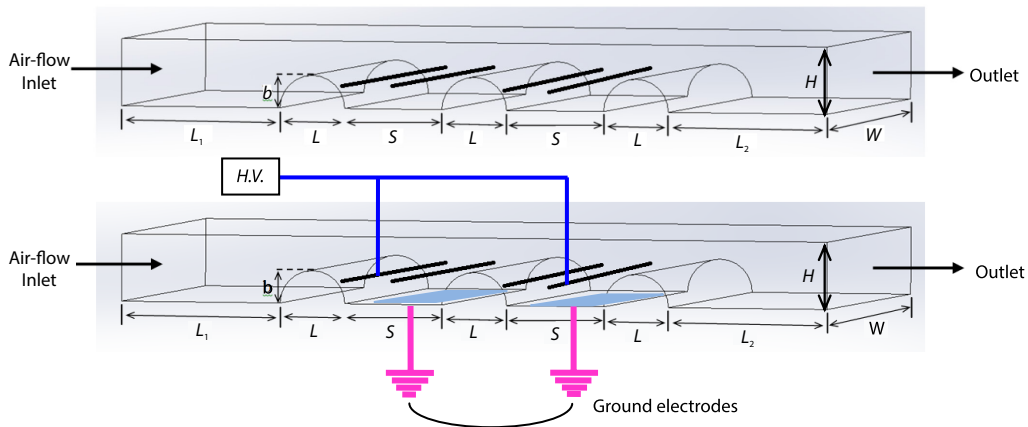


Figure 5. The geometry of 2 cases; (a) plain: Case 1 and (b) active (EHD): Case 2

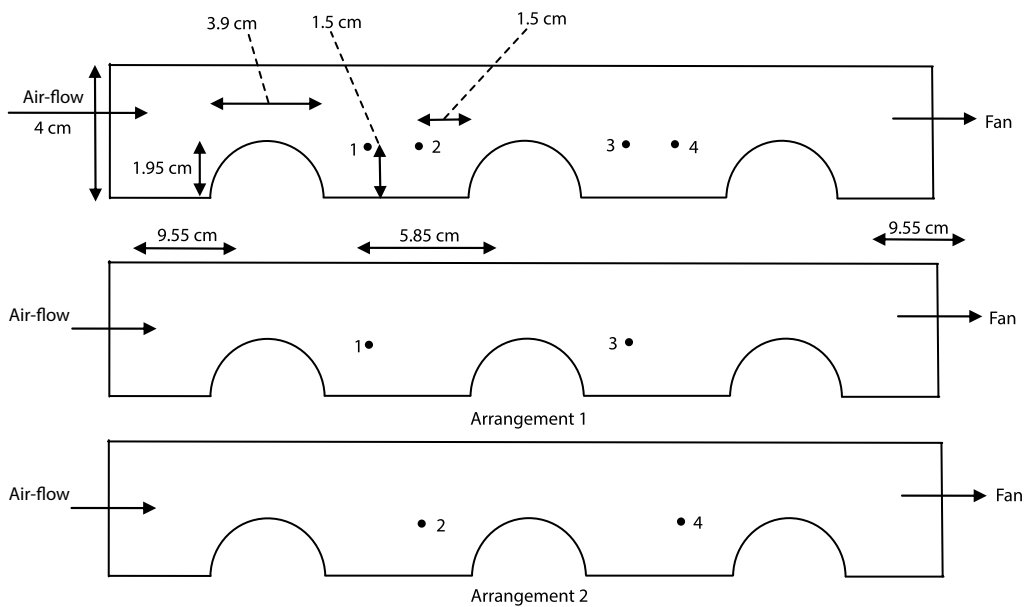


Figure 6. Arrangements of wire electrodes

The arrangement of electrodes with their geometric coding values is illustrated in fig. 6. The arrangements of electrodes for active method are displayed in the Case 2. The wire and ground electrodes were inserted between semi circular ribs to enhancement of heat transfer by means of the secondary flow produced from corona wind of EHD wire-plate actuator.

In active method, the secondary flow of corona wind is from the cold main flow to the hot zone. In conclusion, two kinds of enhancement methods could be beneficial for enhancing of heat transfer from semi circular ribs. The aim of this study is to investigate the heat transfer enhancement of 3-D traverse semi circular ribs placed at the base of the channel.

Three parameters characterize the laminar air-flow with heat transfer:

- local and average rate of heat transfer enhancement, E_t :

$$\text{local} \quad E_t = \frac{h}{h_s} = \frac{(T_w - T_{ref})_s}{(T_w - T_{ref})} \quad \text{with} \quad h = \frac{q''_{rib}}{T_w - T_{ref}} \quad (1)$$

$$\text{average} \quad \bar{E}_t = \frac{\bar{h}}{\bar{h}_s} = \frac{(\bar{T}_w - T_{ref})_s}{(\bar{T}_w - T_{ref})} \quad \text{with} \quad \bar{h} = \frac{q''_{rib}}{\bar{T}_w - T_{ref}} \quad (2)$$

- consumed power ratio

$$E_{lost} = \frac{\Delta P}{\Delta P_s} \quad (3)$$

- local and average performance evaluation criteria (PEC), η_e :

$$\text{local} \quad \eta_e = \frac{E_t}{E_{lost}} \quad (4)$$

$$\text{average} \quad \bar{\eta}_e = \frac{\bar{E}_t}{\bar{E}_{lost}} \quad (5)$$

In the sequence of eqs. (1)-(5), q''_{rib} is the constant heat flux from semi circular ribs to fluid-flow, h – the local heat transfer coefficient, T_{ref} – the reference temperature (inlet temperature to the test section), T_w – the temperature of surface of semi circular ribs in floor of test section, including surface of semi circular ribs and spacing of them, ΔP – the pressure loss, and subscript s denotes the plain case without enhancement intervention. The Re_{D_h} is Reynolds number based on the hydraulic diameter of the channel, N_{EHD} is EHD number. The N_{EHD} is defined:

$$N_{EHD} = \frac{\rho_e E_0^2 L^2}{\rho_f \nu_f^2} = \frac{b E_0 L}{\nu_f} = \frac{u_i L}{\nu_f} \quad (6)$$

This parameter is similar to the Re_{D_h} number based on velocity of electric ions and with the assumption of similar density for ions and neutral fluid particles. In eq. (6), ρ_e is density of electric charge, ρ_f is density of fluid, E_0 is electric field, b is mobility of ions, and ν_f is the kinematics viscosity of fluid. is defined:

$$u_i = \frac{I_0}{q_{e0}} \quad (7)$$

In this equation, I_0 is electric current of corona wind, q_{e0} – electric charge of one electron, which is $1.602 \cdot 10^{-19}$ Coulomb. The L is the characteristic length and defined as [15]:

$$L = D_h \alpha \frac{C}{H} \ln \frac{r_{eff}}{r} \quad (8)$$

where α is the view angle between wire and ground electrodes ($\alpha = 1$ for the case of one wire electrode between two ground electrodes and $\alpha = 0.5$ for the case of one wire and one ground electrode). The C/H is the ratio of space of wire and ground electrodes to channel height, r_{eff}/r – the ratio of effective radius of wire and ground electrodes to the radius of wire electrode, and r_{eff} is defined as $r_{\text{eff}} = 4C/\pi$, where C – the distance between wire and ground electrodes.

Results and discussion

The geometry of semi circular ribs arrangements as illustrated in fig. 5 are: $L_1 = L_2 = 110$ mm, $L = 30$ mm, $S = 30$ mm, $b = 20$ mm, and $H = 40$ mm. As it is seen in fig. 7, the distribution of wall temperature for the plain case (without EHD, $Re_{Dh} = 500-4500$) is shown.

In fig. 8, the rate of heat transfer enhancement for forced convection ($Re_{Dh} = 500-4500$) is shown. The effect of forced convection on heat transfer enhancement depending on the Reynolds number was shown in the figures. In reference to this figure, the local and average heat transfer enhancement has been increased as a consequence of increments in Reynolds number. The impact of Reynolds number on the heat transfer enhancement was seen in the figure. Herein, the local and average heat transfer enhancement for $Re_{Dh} = 4500$ is higher than their counterparts for others.

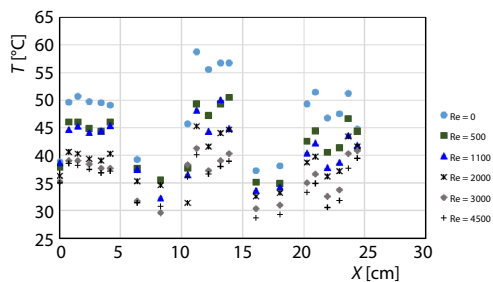


Figure 7. Wall temperature distribution in direction of rib's surface for forced convection

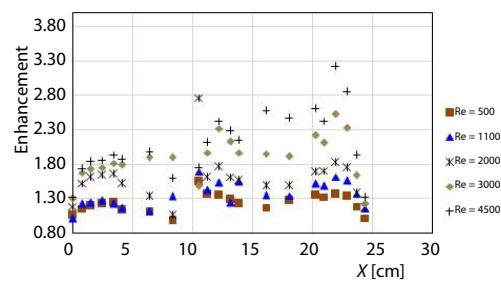


Figure 8. Comparison of rate of heat transfer enhancement in direction of rib's surface for forced convection ($Re_{Dh} = 500-4500$)

In figs. 9 and 10, the rate of heat transfer enhancement for $Re_{Dh} = 10$ (without fan) in Arrangements 1 and 2 with voltages of 9 kV, 12 kV, and 15 kV is shown. The effect of voltage on heat transfer enhancement depending on the wire arrangement was shown in the figures. In reference to these figures, the local and average heat transfer enhancement has been increased as a consequence of increments in voltage. The density of electric charge around of wire elec-

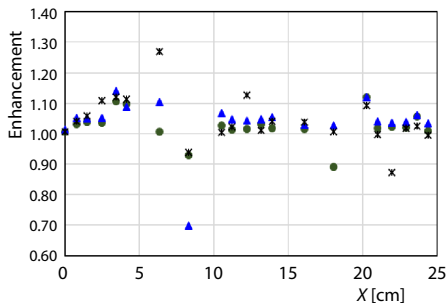


Figure 9. Comparison of rate of heat transfer enhancement in direction of rib's surface for Arrangement 1 (9 kV, 12 kV, and 15 kV; $Re_{Dh} = 0$)

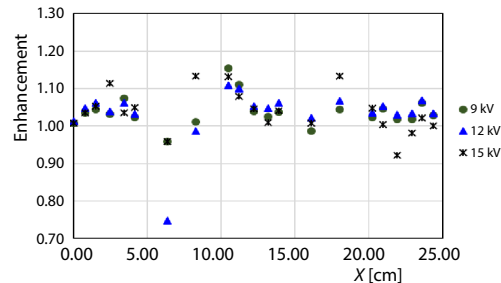


Figure 10. Comparison of rate of heat transfer enhancement in direction of rib's surface for Arrangement 2 (9 kV, 12 kV, and 15 kV; $Re_{Dh} = 0$)

trode in Arrangement 1 is higher than that in Arrangement 2. Therefore, Arrangement 1 is better than Arrangement 2.

As it is seen in figs. 11 and 12, the rate of heat transfer enhancement for $Re_{D_h} = 500$ and active EHD case in Arrangements 1 and 2 with voltages of 9 kV, 12 kV, and 15 kV is shown. The effect of voltage on heat transfer enhancement depending on the wire Arrangement was shown in the figures. In reference to these figures, the local and average heat transfer enhancement has been increased as a consequence of increments in voltage. The density of electric charge around of wire electrode in Arrangement 1 is higher than that in Arrangement 2. Therefore, Arrangement 1 is better than Arrangement 2.

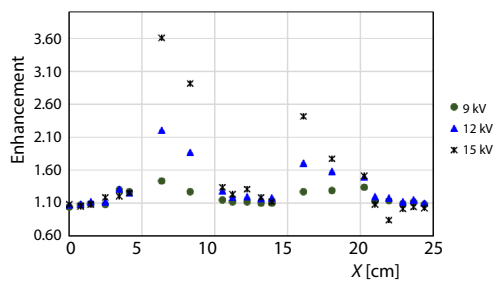


Figure 11. Comparison of rate of heat transfer enhancement in direction of rib's surface for Arrangement 1 (9 kV, 12 kV, and 15 kV; $Re_{D_h} = 500$)

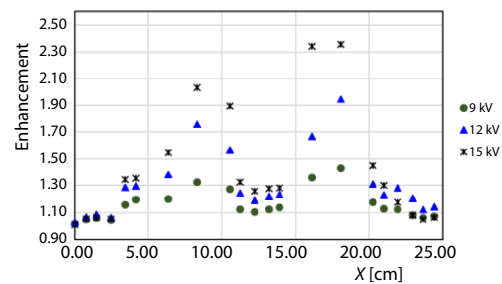


Figure 12. Comparison of rate of heat transfer enhancement in direction of rib's surface for Arrangement 2 (9 kV, 12 kV, and 15 kV; $Re_{D_h} = 500$)

As it is seen in figs. 13 and 14, the rate of heat transfer enhancement for $Re_{D_h} = 4500$ and active EHD case in Arrangements 1 and 2 with voltages of 9 kV, 12 kV, and 15 kV is shown. The effect of voltage on heat transfer enhancement depending on the wire arrangement was shown in the figures. In reference to these figures, the local and average heat transfer enhancement has been increased as a consequence of increments in voltage. The density of electric charge around of wire electrode in Arrangement 1 is higher than that in Arrangement 2. Therefore, Arrangement 1 is better than Arrangement 2.

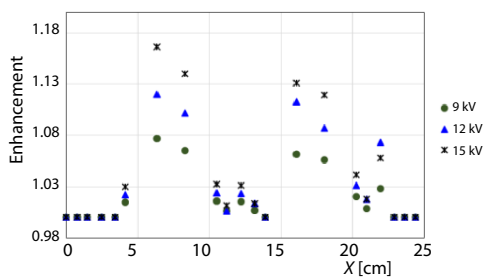


Figure 13. Comparison of rate of heat transfer enhancement in direction of rib's surface for Arrangement 1 (9 kV, 12 kV, and 15 kV; $Re_{D_h} = 4500$)

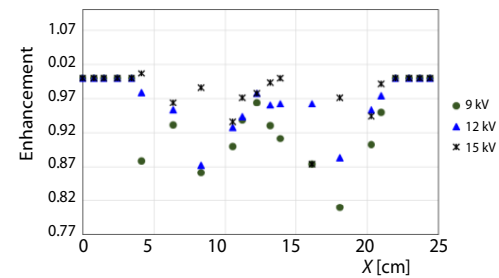


Figure 14. Comparison of rate of heat transfer enhancement in direction of rib's surface for Arrangement 2 (9 kV, 12 kV, and 15 kV; $Re_{D_h} = 4500$)

The semi circular ribs are heated with constant heat flux and therefore for comparison of EHD active method, the plain case (without EHD, $Re_{D_h} = 4500$) is base. In figs. 11-14, the effects of EHD active method on heat transfer enhancement and the temperature reduction are

shown in test section. In the space between the semi circular ribs, the insulator (incombustible fiber) has been applied and adiabatic boundary condition brings a temperature reduction. The effect of voltage on heat transfer enhancement depends on the wire arrangement as shown in these figures. It is clear from the figures, that the local and average heat transfer enhancement was increased with increments in voltage. Therefore, the Arrangement 1 is better than Arrangement 2. The impact of Reynolds number on the heat transfer enhancement was seen in these figures. Herein, the local and average heat transfer enhancement for $Re_{D_h} = 500$ is higher than their counterparts for other Reynolds numbers. For high Reynolds numbers, the power of the main flow is higher than the power of corona wind (secondary flow) in the main flow eliminating the effects of corona wind.

The power of corona wind in the case of low Reynolds numbers is higher than in the case of high Reynolds numbers. Consequently, the corona wind in low Reynolds numbers affects the main flow better than in situations of high Reynolds numbers. Inspection of the figure reveals that the average heat transfer enhancement has been increased with elevations in voltage. At high voltages, the density of electric charge and the electric field around of wire electrodes is high. This is interpreted in terms of the corona wind, which at high voltages has a direct influence on the main flow better than those situations of low voltages.

As it is seen in fig. 15, comparison of the average rate of heat transfer enhancement in various Reynolds numbers with arrangements 1, 2 for 12 kV is shown. It is clear from this figure, that the average heat transfer enhancement was decreased with increments in Reynolds numbers. With attention to fig. 14, attests that the density of electric charge around of wire electrode in Arrangement 1 is higher than that in Arrangement 2. As a consequence, Arrangement 1 is better than Arrangement 2.

In fig. 16, the variations of $\bar{\eta}_e$ with Reynolds number for active method of heat transfer enhancement in $Re_{D_h} = 500, 1100, 2000, 3000,$ and 4500 are presented. As seen in figure, the effect of Reynolds number on heat transfer enhancement for active method demonstrates the opposite behavior for both low and high values. For the active method, the secondary flow can move further to the spacing between ribs. With attention to fig. 15, attests that the pressure loss around of wire electrode in Arrangement 1 is higher than that in Arrangement 2. As a consequence, Arrangement 2 is better than Arrangement 1. Also in $Re_{D_h} = 4500$, it is detected that for positive interaction of the average heat transfer enhancement and consumed power ratio (ratio of pressure loss) seems to be better than others Reynolds numbers.

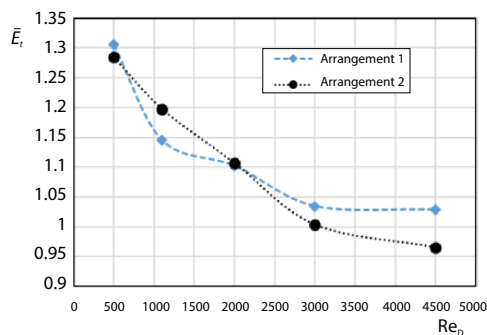


Figure 15. Comparison of the average rate of heat transfer enhancement in various Reynolds numbers with Arrangements 1, 2 for 12kV

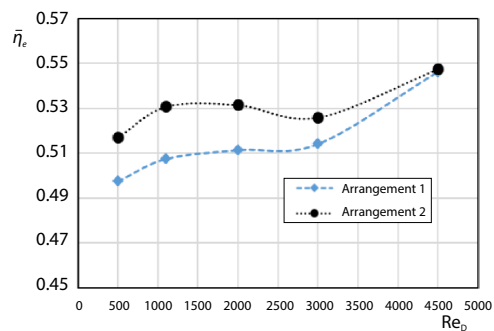


Figure 16. The average PEC in various Reynolds numbers with Arrangements 1, 2 for 12 kV

The uncertainty analysis for E_t , η_e , \bar{E}_t , and $\bar{\eta}_e$ has been carried out too. The uncertainty for local quantities of E_t and η_e is smaller than 8.5% and for average quantities of \bar{E}_t and $\bar{\eta}_e$ is 3.8-5% [16]. In fig. 17 the uncertainty analysis for various temperature points obtained from one sample of iterative tests is presented. In fig. 18 the uncertainty analysis for various E_t points obtained from one sample of iterative tests is presented. The values of uncertainty analysis with error calculation have been achieved in tab. 1. This table show that the parameters pressure, velocity, temperature, \bar{E}_t and $\bar{\eta}_e$.

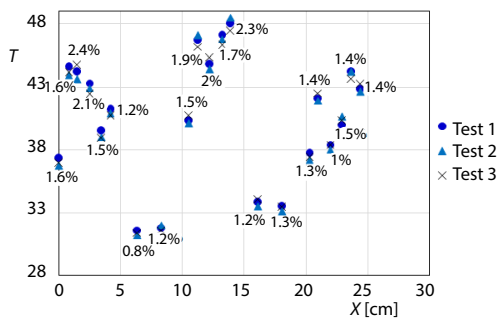


Figure 17. Uncertainty analysis in various temperature points obtained from one sample of iterative tests

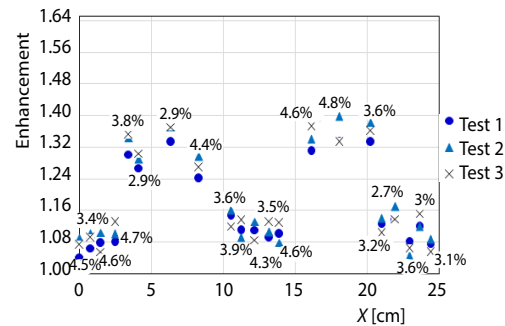


Figure 18. Uncertainty analysis in various E_t points obtained from one sample of iterative tests

Table 1. Average uncertainty analysis of all measured parameters

	P (pressure)	V (velocity)	T (temperature)	\bar{E}_t	$\bar{\eta}_e$
% Error	3.5	3	1.54	3.8	5

Conclusions

This study has been achieved the enhancement of heat transfer from semi circular ribs in a channel flow using an active method. The new parameter η_e has been introduced. The parameter η_e of deals with the simultaneous effects of heat transfer enhancement and consumed power ratio (the pressure loss ratio) on the cooling performance. The following conclusions from the experimental study are listed.

- The power of corona wind (secondary flow) in low Reynolds number flows is higher than in high Reynolds number flows, signifying that the corona wind in low Reynolds numbers is better than in high Reynolds numbers.
- The active method for low Reynolds numbers with laminar flows is advantageous. The average and local heat transfer enhancement climbs up to 143.9% and 360%, respectively.
- For the same Reynolds numbers and wire arrangements, the heat transfer enhancement was increased with increments in voltage of the wire electrodes. At high voltages, the density of electric charge and the electric field around of wire electrodes is high. Therefore, the corona wind in high voltages has been effect on main flow better than low voltages.
- In same Reynolds numbers and voltages of wires, the heat transfer enhancement was increase in Arrangement 1 than Arrangement 2. Density of electric charge around of wire electrodes in Arrangement 1 is higher than Arrangement 2. Therefore, the Arrangement 1 is better than Arrangement 2.
- Active method for low Reynolds numbers has higher average PEC equal to 0.548. The power of corona wind in low Reynolds number is higher than high Reynolds number. With

decrements in the laminar Reynolds number, the interaction strength of EHD secondary flow was increased. In turbulent Reynolds numbers, the interaction strength of EHD flow was decreased. Therefore, the corona wind in low Reynolds numbers has been affect on main flow better than high Reynolds numbers.

Nomenclature

b – mobility of ions, [$\text{m}^2\text{V}^{-1}\text{s}^{-1}$]
 C – distance between wire and ground electrodes, [m]
 D – diameter of pipe, [m]
 D_h – hydraulic diameter ($=2WH/W+H$), [m]
 d – ratio in diameter
 E_t – heat transfer enhancement ratio
 $[= h/h_s = (T_w - T_{ref})_s / (T_w - T_{ref})]$
 E_{lost} – consumed power ratio ($= \Delta P / \Delta P_s$)
 E_0 – electric field, [Vm^{-1}]
 H – channel height, [m]
 h – heat transfer coefficient, [$\text{W}\text{m}^{-2}\text{K}^{-1}$]
 h_s – heat transfer coefficient for plain case, [$\text{W}\text{m}^{-2}\text{K}^{-1}$]
 I_0 – electric current of corona wind, [A]
 L – width of semi circular rib, characteristic length, [m]
 L_1 – length of upstream region, [m]
 L_2 – length of downstream region, [m]
 N_{EHD} – EHD number ($= u_i L / \nu_j$)
 P – pressure, [Pa]
 q''_{rib} – constant heat flux from semi circular rib, [Wm^{-2}]
 q_{e0} – electric charge of one electron, [Coulomb]
 Re – Reynolds number ($= VD\nu^{-1}$)
 Re_{Dh} – Reynolds number based on hydraulic diameter ($= VD_h \nu^{-1}$)
 r – radius of wire electrode, [m]
 r_{eff} – effective radius of wire to ground electrode, [m]

S – separation between semi circular ribs, [m]
 T – temperature, [K, °C]
 u_i – velocity of electric ions, [ms^{-1}]
 v – velocity
 W – width of channel, [m]
 x, y, z – Cartesian co-ordinates

Greek symbols

α – view angle between wire and ground electrodes
 η_e – performance evaluation criteria (PEC)
 ν – kinematics viscosity, [m^2s^{-1}]
 ρ_f – density of fluid
 ρ_e – density of electric charge
 Δ – difference

Subscripts

e – electron
 f – fluid
 i – ions
 ref. – reference condition
 s – plain case
 W – semi circular rib wall

Superscripts

" – flux
 – – average

References

- [1] Alamgholilou (Alami nia), A., Esmailzadeh, E., Experimental Investigation on Hydrodynamics and Heat Transfer of Fluid Flow into Channel for Cooling of Rectangular Ribs by Passive and EHD Active Enhancement Methods, *Journal Experimental Thermal and Fluid Science*, 38 (2012), Apr., pp. 61-73
- [2] Alamgholilou (Alami nia), A., Esmailzadeh, E., Numerical Investigation on Effects of Secondary Flow into Duct for Cooling of the Ribs by Passive Enhancement Method, *Journal Enhanced Heat Transfer*, 19 (2008), 3, pp. 233-248
- [3] Esmailzadeh, E., Alamgholilou (Alami nia), A., Numerical Investigation of Heat Transfer Enhancement of Rectangular Ribs with Constant Heat Flux Located in the Floor of a 3-D Duct Flow, *Asian J. Applied Sciences*, 1 (2008), 4, pp. 286-303
- [4] Alami nia, A., Campo, A., Experimental Investigation on Flow and Heat Transfer for Cooling Flush-Mounted Ribbons in a Channel-Application of an Electrohydrodynamics Active Enhancement Method, *Journal Thermal Science*, 20 (2016), 2, pp. 505-516
- [5] Alami nia, A., Campo, A., Experimental Study on EHD Heat Transfer Enhancement from Flush-Mounted Ribbons with Different Arrangements of Wire Electrodes in a Channel, *Heat Mass Transfer*, 52 (2016), 12, pp. 2823-2831
- [6] Sultan, G. I., Enhancing Forced Convection Heat Transfer from Multiple Protruding Heat Sources Simulating Electronic Components in a Horizontal Channel by Passive Cooling, *Microelectronics Journal*, 31 (2000), 9-10, pp. 773-779

- [7] Fujishima, H., *et al.*, Numerical Simulation of Three-Dimensional EHD of Spiked-Electrode Electrostatic Precipitators, *IEEE*, 13 (2006), 1, pp. 160-167
- [8] Ohadi, M. M., *et al.*, Heat Transfer Enhancement of Laminar and Turbulent Pipe Flow via Corona Discharge, *Int. Journal of Heat and Mass Transfer*, 34 (1991), 4-5, pp. 1175-1187
- [9] Kasayapanand, N., Kiatsiriroat, T., EHD Enhanced Heat Transfer in Wavy Channel, *International Communications in Heat and Mass Transfer*, 32 (2005), 6, pp. 809-821
- [10] Kasayapanand, N., Kiatsiriroat, T., Optimized Electrode Arrangement in Solar Air Heater, *Renewable Energy*, 31 (2006), 4, pp. 439-455
- [11] Kasayapanand, N., *et al.*, Effect of the Electrode Arrangements in a Tube Bank on the Characteristic of Electrohydrodynamic Heat Transfer Enhancement: Low Reynolds Number, *Journal Enhanced Heat Transfer*, 9 (2002), 5-6, pp. 229-242
- [12] Shooshtari, A., *et al.*, Experimental and Numerical Analysis of Electrohydrodynamic Enhancement of Heat Transfer in Air Laminar Channel Flow, *Proceedings*, 19th Annual IEEE Semiconductor Thermal Measurement and Management Symposium, San Jose, Cal., USA, 2003, pp. 48-52
- [13] Tada, Y., *et al.*, Heat Transfer Enhancement in a Convective Field by Applying Ionic Wind, *Journal Enhanced Heat Transfer*, 4 (1997), 2, pp. 71-86
- [14] ***, Measurement of Fluid Flow by Means of Orifice Plates, Nozzles and Venturi Tubes, Standard French, NF X 10-102, 1971
- [15] Goo, J. H., Le, J. W., Stochastic Simulation of Particle Charging and Collection Characteristics for Wire-Plate Electrostatic Precipitator of Short Length, *Journal Aerosol Science*, 28 (1997), 5, pp. 875-893
- [16] Moffat, R. J., Describing the Uncertainties in Exp. Results, *Exp. Thermal & Fluid Science*, 1 (1988), 1, pp. 3-17